Human Molecular Genetics, 2012, Vol. 21, No. 26 ***5443–5455***
doi:10.1093/hmg/dds390
Advance Access published on September 26, 2012

A novel FGFR3-binding peptide inhibits FGFR3 signaling and reverses the lethal phenotype of mice mimicking human thanatophoric dysplasia

Min Jin[1], Ying Yu[2], Huabing Qi[1], Yangli Xie[1], Nan Su[1], Xiaofeng Wang[1], Qiaoyan Tan[1], Fengtao Luo[1], Ying Zhu[1], Quan Wang[1], Xiaolan Du[1], Cory J. Xian[3], Peng Liu[1], Haiyang Huang[1], Yue Shen[1], Chu-Xia Deng[4], Di Chen[5] and Lin Chen[1,*]

[1]Center of Bone Metabolism and Repair, State Key Laboratory of Trauma, Burns and Combined Injury, Institute of Surgery Research, Daping Hospital, Third Military Medical University, Chongqing 400042, China, [2]School of Pharmacy and Bioengineering, Chongqing University of Technology, Chongqing 400050, China, [3]Sansom Institute for Health Research, School of Pharmacy and Medical Sciences, University of South Australia, Adelaide, SA 5001, Australia, [4]Genetics of Development and Disease Branch, National Institute of Diabetes, Digestive and Kidney Diseases, US National Institutes of Health, 10 Center Drive, Bethesda, MD 20892, USA and [5]Department of Biochemistry, Rush University Medical Center, 1735 West Harrison Street, Chicago, IL 60612-3823, USA

Received May 19, 2012; Revised September 3, 2012; Accepted September 14, 2012

Gain-of-function mutations in fibroblast growth factor receptor-3 (FGFR3) lead to several types of human skeletal dysplasia syndromes including achondroplasia, hypochondroplasia and thanatophoric dysplasia (TD). Currently, there are no effective treatments for these skeletal dysplasia diseases. In this study, we screened, using FGFR3 as a bait, a random 12-peptide phage library and obtained 23 positive clones that share identical amino acid sequences (VSPPLTLGQLLS), named as peptide P3. This peptide had high binding specificity to the extracellular domain of FGFR3. P3 inhibited tyrosine kinase activity of FGFR3 and its typical downstream molecules, extracellular signal-regulated kinase/mitogen-activated protein kinase. P3 also promoted proliferation and chondrogenic differentiation of cultured ATDC5 chondrogenic cells. In addition, P3 alleviated the bone growth retardation in bone rudiments from mice mimicking human thanatophoric dysplasia type II (TDII). Finally, P3 reversed the neonatal lethality of TDII mice. Thus, this study identifies a novel inhibitory peptide for FGFR3 signaling, which may serve as a potential therapeutic agent for the treatment of FGFR3-related skeletal dysplasia.

INTRODUCTION

Longitudinal bone growth is achieved at the growth plate where a cartilaginous template is made and then is converted to trabecular bone at the adjacent metaphysis, a process called endochondral ossification (1). In 1990s, gain-of-function mutations in fibroblast growth factor receptor-3 (FGFR3) were found responsible for achondroplasia (ACH), the most common type of human dwarfism (2,3). Later on, gain-of-function mutations in FGFR3 were further identified in several other types of human skeletal dysplasias, including hypochondroplasia (HCH) and thanatophoric dysplasia (TD) (4). TD has been classified into TDI and TDII. TDI patients have curved, short femurs with or without cloverleaf skull and TDII patients have relatively longer femurs with severe cloverleaf skull (5). In contrast, humans with downregulated FGFR3 activity exhibit camptodactyly, a syndrome with a tall stature, scoliosis and hearing loss (CATSHL) (6). These studies demonstrate that FGFR3 is a negative regulator of endochondral bone growth.

Mice carrying activated mutations in FGFR3 are obviously small, with smaller round heads, shorter long bones and abnormal morphologic structure of growth plates (7–9). It has been demonstrated that FGFR3 inhibits chondrocyte proliferation

*To whom correspondence should be addressed. Tel: +86 2368702991; Fax: +86 2368702991; Email: linchen70@163.com

through Stat1 signaling by inducing the expression of cell cycle suppressor genes, such as the cyclin-dependent kinase inhibitor p21 (10–12). Moreover, FGFR3 also inhibits chondrocyte differentiation via the extracellular signal-regulated kinase (ERK)/mitogen-activated protein kinase (MAPK) pathway (13).

Although these studies have significantly improved our understanding of the mechanisms for FGFR3-related skeletal dysplasia, no effective treatments for these genetic skeletal disorders are now available. It is conceivable that downregulating the activity of FGFR3 itself or its downstream molecules may alleviate the skeleton phenotypes of ACH/TD. In the present study, we screened a phage library containing random 12-peptide inserts, using FGFR3 as bait, and obtained 23 positive clones that share identical amino acid sequences (VSPPLTLGQLLS), named as peptide P3. P3 had high binding affinity to the extracellular domain of FGFR3. We found that P3 inhibited the tyrosine kinase activity of FGFR3 and its downstream ERK/MAPK pathway in chondrocytes. P3 also promoted proliferation and chondrogenic differentiation of cultured ATDC5 chondrogenic cells. In addition, P3 improved the growth of bone rudiments from TDII mice *in vitro* and rescued the lethal phenotype of mice mimicking human TDII *in vivo*.

RESULTS

Identification of specific FGFR3-binding peptide using phage display technique

Three rounds of biopanning were performed to select specific FGFR3-binding clones from the 12-peptide phage library. As shown in Table 1, phage recovery rates of the second and third round of screening were much higher than the first round (4.44×10^{-5}% and 4.66×10^{-3}% compared with 2.99×10^{-2}%), indicating that phages with a high affinity to FGFR3 were effectively enriched after three rounds of selection (Table 1). A total of 44 individual phage clones were obtained after three rounds of panning. Their corresponding amino acid sequences were deduced from the DNA sequences. Among 44 phage clones, 23 clones shared identical amino acid sequences (VSPPLTLGQLLS, named as peptide P3).

To identify high-affinity FGFR3-binding clones, the recovered phage clones were examined by enzyme-linked immunosorbent assay (ELISA) for FGFR3 binding with control phage (vcsM13) (Fig. 1A). When optical density (OD) values of phage clones were two times greater than that of phage vcsM13, they will be considered to have high binding affinity for FGFR3. As shown in Figure 1A, OD values of four selected clones with different amino acid sequences (the phage clone 3 having P3 sequence) were five times higher than that of the control, indicating that these four clones had high binding affinity to FGFR3.

We next tested their ability to bind FGFR3 through competitive elution with FGF2 (Fig. 1B). Our data indicated that FGF2 had high elution efficiency for these clones, especially for clones 1–3 (over 96%). Since FGF2 exerts its biological activities via binding to the extracellular domain of FGFR3 (14), the competitive binding of these phage clones with FGF2 to FGFR3 suggests that these phage clones may mimic the binding of FGF2 to the extracellular domain of FGFR3.

Table 1. Enrichment of phages with a high FGFR3 binding affinity

	Input phages (pfu)	Output phages (pfu)	Recovery[a] (%)
Round 1	2×10^{11}	8.87×10^{4}	4.44×10^{-5}
Round 2	2.06×10^{11}	9.60×10^{6}	4.66×10^{-3}
Round 3	2.1×10^{11}	6.28×10^{7}	2.99×10^{-2}

pfu, plaque forming unit.
[a]Recovery (%) = (Output phages/Input phages) × 100%.

Peptide P3 binds specifically to the extracellular domain of FGFR3

To assess the binding ability and specificity of P3 to FGFR3, ELISA binding studies were performed (15). In this assay, P3 peptide was coated on the plate, the extracellular or intracellular fragment of FGFR3 was then added and the bound FGFR3 protein was detected by corresponding specific antibody following enzymatic color reaction as facilitated by a secondary antibody conjugated with horseradish peroxidase (HRP) and absorbance reading. To determine which region of FGFR3 has been bound by P3, we tested the dose–response effect of P3 to bind the extracellular or intracellular fragment of FGFR3. The results of binding assays demonstrated that P3 strongly bound to the extracellular region of FGFR3, but not the intracellular domain of FGFR3 (Fig. 1C).

Peptide P3 inhibits tyrosine kinase activity of FGFR3

To determine whether P3 affects FGFR3 activity, we first investigated the effect of peptide P3 on FGFR3 tyrosine kinase activity. Wild-type (WT) and constitutively active mutant FGFR3 (FGFR3 K650M, FGFR3 K644E) were transiently expressed in 293T cells, and the cells were then treated with or without 10 μM of P3. The results showed that peptide P3 significantly inhibited the phosphorylation of WT FGFR3, K650M FGFR3 and K644E FGFR3, indicating that peptide P3 had the ability to inhibit ligand-independent activation of FGFR3 (Fig. 2A).

Peptide P3 inhibits the ERK/MAPK pathway in FGFR3-expressing chondrocytic cell line ATDC5

We next examined the effects of P3 on downstream signaling of FGFR3 in ATDC5 cells that have strong expression of FGFR3 (16). Since FGFs/FGFRs exert their diverse biological effects through multiple intracellular signaling pathways, among which the ERK/MAPK pathway has been found to inhibit chondrocyte differentiation and matrix synthesis (13), we examined the effect of P3 on ERK1/2 phosphorylation induced by FGF2 in the ATDC5 cells. Our data showed that the FGF2-mediated ERK1/2 phosphorylation was partially blocked by P3 at different time points after FGF2 treatment (Fig. 2B), indicating that peptide P3 inhibited FGFR3 downstream signaling, the ERK/MAPK pathway in chondrocytes.

Peptide P3 promotes chondrocyte proliferation and differentiation

ATDC5 cell line is an appropriate *in vitro* model for studying chondrogenesis (17). Methylthiazoletetrazolium (MTT) assay was used to test the concentration-dependent effect of peptide P3 treatment (for 24 h) on ATDC5 proliferation. We found that P3 significantly increased ATDC5 cells proliferation (Fig. 3A). In the presence of FGF2 in culture, P3 significantly reversed the inhibitory effect of FGF2 on ATDC5 proliferation (Supplementary Material, Fig. S1A). To examine the apoptotic effect of P3 on ATDC5 cells, we performed a terminal deoxynucleotidyl transferase dUTP nick end-labeling assay and found that treatment with P3 (10 μM) had no significant effect on the apoptosis of ATDC5 cells (Supplementary Material, Fig. S1B). To determine whether P3 rescued FGFR3 signal-mediated inhibition on chondrogenesis, we added P3 (10 μM) to the ATDC5 cell micromass cultures treated with FGF2 (20 ng/ml). The abundance of sulfated proteoglycans was grossly revealed by Alcian blue staining. The staining intensity was significantly reduced in FGF2-treated cells. Addition of P3 at the beginning of the chondrogenic induction period significantly reversed the inhibitory effect of FGF2 on chondrogenesis since similar staining intensity was observed in cells treated with FGF2 plus P3 or cells treated with P3 alone when compared with the controls (Fig. 3B). Levels of sulfated glycosaminoglycans (Fig. 3C), as quantified by Dimethylmethylene Blue (DMMB) assay, were significantly decreased in FGF2-treated ATDC5 micromass culture compared with nontreatment controls. Addition of P3 significantly increased sulfated glycosaminoglycans in FGF2-treated ATDC5 micromass cultures, with the levels of glycosaminoglycans not significantly different from those of FGF2-nontreated controls. These results were consistent with the results of Alcian blue staining. These results suggest that P3 prevented the inhibitory effect of FGF2 on chondrocyte differentiation.

We further determined the effect of P3 on the expressions of several chondrogenic marker genes during ATDC5 differentiation with P3 (10 μM) being added from the beginning of the chondrogenic induction. After 3 or 7 days incubation, total RNA was extracted and real-time polymerase chain reaction (PCR) analysis was performed. We found that the levels of several chondrogenic markers, such as *Sox9*, *Col2* and *Col10*, were all increased in cultures treated with P3 peptide when compared with nontreated controls (Fig. 3D–F). The levels of *Col2* mRNA were up-regulated approximately by 40% at Day 3 and by 51% at Day 7 in P3-treated cells. The levels of *Sox9* mRNA were increased by 100% at Day 3, and by 225% at Day 7. There was a minor increase in *Col10* levels at Day 3 and ~34% increase in *Col10* levels at Day 7. These results indicate that peptide P3 promoted the chondrogenic differentiation.

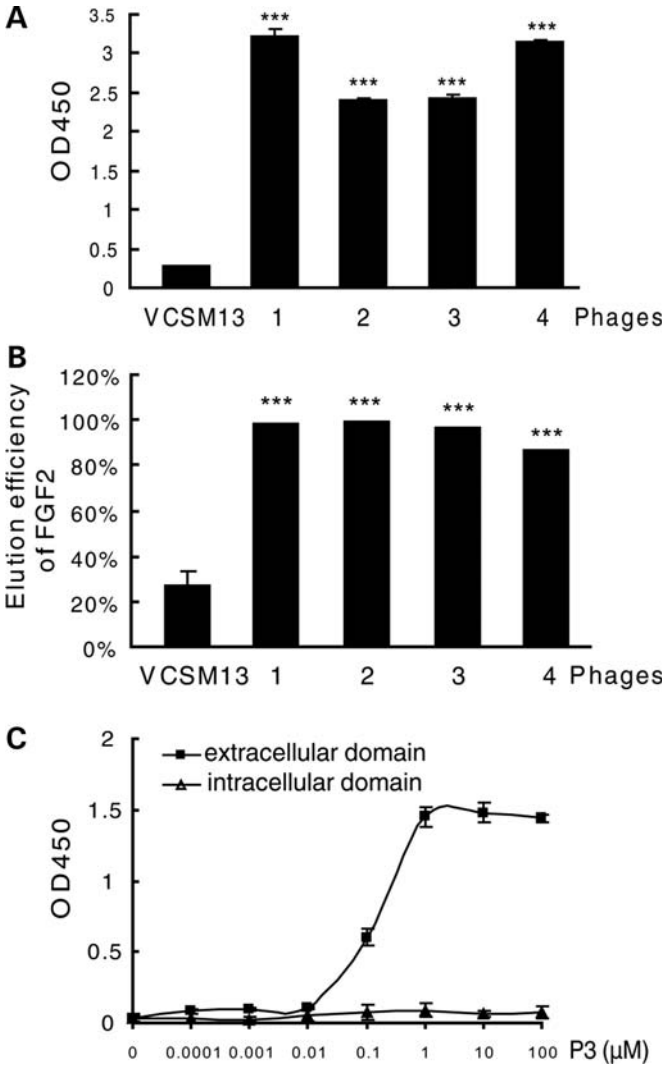

Figure 1. Specific binding of the positive phage clones to FGFR3. (**A**) The binding affinity to FGFR3 of four selected positive phage clones and the control vcsM13 was determined by ELISA assay ($n = 3$, $^{***}P < 0.001$, versus VCSM13). (**B**) Detection of FGF2 elution efficiency to the four selected positive phage clones. The elution efficiency of FGF2 is calculated as follows: (the OD_{450} value of the phage binding to FGFR3 before competitive elution with FGF2 − the OD_{450} value of the phage remaining binding to FGFR3 after competitive elution with FGF2)/the OD_{450} value of the phage binding to FGFR3 before competitive elution with FGF2. ($n = 3$, $^{***}P < 0.001$, versus VCSM13). (**C**) Affinity detection of peptide P3 binding to FGFR3 by ELISA. Increasing amounts of P3 were immobilized and incubated with the extracellular region or the intracellular region of human FGFR3 protein. Specific binding was detected using antibodies against the extracellular region and the intracellular region of human FGFR3, respectively.

Peptide P3 attenuates FGFR3-mediated growth inhibition in metatarsal bones cultures

To determine the effect of P3 on FGFR3-mediated inhibition of bone development, we employed an embryonic bone culture system, in which bone growth can be monitored under defined conditions. We examined the effects of P3 on the growth of the cultured metatarsal bones isolated from developing embryos of mice mimicking human TDII (*Fgfr3*$^{Neo-K644E/+}$ EIIa-Cre mice) (18). The growth of rudiments was evaluated by calculating the percentage increase of length before and after culture with or without P3 treatment. The percentage increases in total length (TL) of bone and the length of hypertrophic zone of metatarsals from TDII mice were smaller compared with WT mice, further confirming the FGFR3-mediated inhibition of bone growth and chondrocyte differentiation (Fig. 4A–C). Cultures of bones from

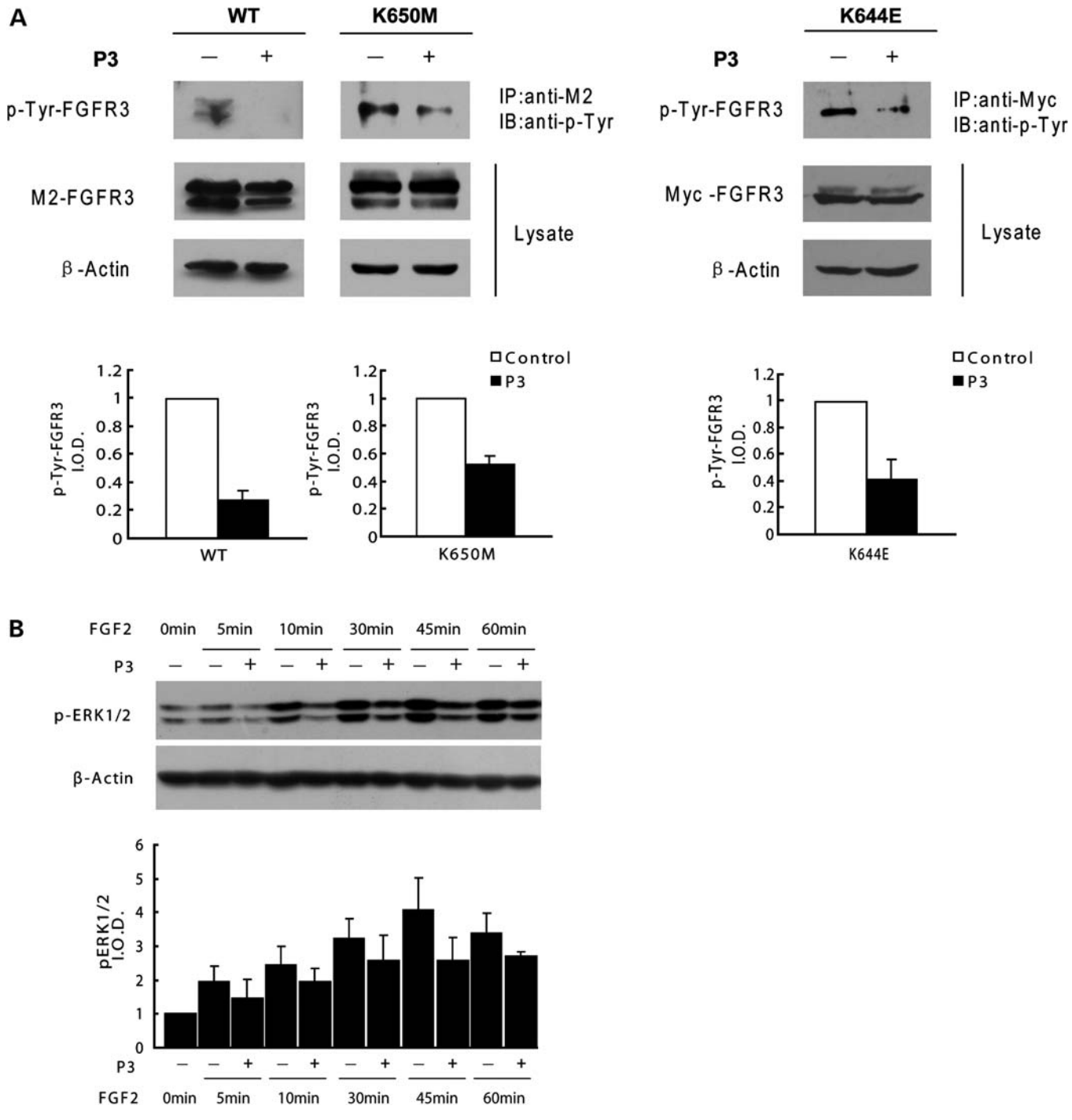

Figure 2. Peptide P3 inhibits FGFR3 signaling. (**A**) Peptide P3 inhibits tyrosine kinase activation of FGFR3. WT, K650M and K644E mutant of FGFR3 were transiently expressed in 293T cells, lysed and immunoprecipitated with an anti-M2 antibody or anti-Myc antibody. Blots were then incubated with an anti-phospho-tyrosine antibody. Phospho-tyrosine band signal intensity was quantified by densitometry. The error bars indicate the standard deviation (SD) from three separate experiments. (**B**) Peptide P3 inhibits the FGF2-mediated ERK/MAPK phosphorylation in FGFR3-expressing chondrocytic cell line ATDC5. Western blot analysis demonstrated that the levels of phospho-ERK1/2 induced by FGF2 (20 ng/ml) were down-regulated by P3 (10 μM) in ATDC5 cells. The levels of phospho-ERK1/2 were quantified by densitometry.

TDII embryos for 7 days revealed that treatment with 10 μM of P3 increased the TL of metatarsal bone compared with non-treated controls (Fig. 4A and B). Quantitative analysis also revealed that the percentage increase in the length of hypertrophic zone of TDII bones was also increased by P3 treatment (Fig. 4C). However, P3 had no significant effect on the percentage increase in the length of proliferative zone of TDII bones (Fig. 4D). Our data indicate that peptide P3 alleviated the bone growth retardation mainly by promoting chondrocyte differentiation in TDII mice.

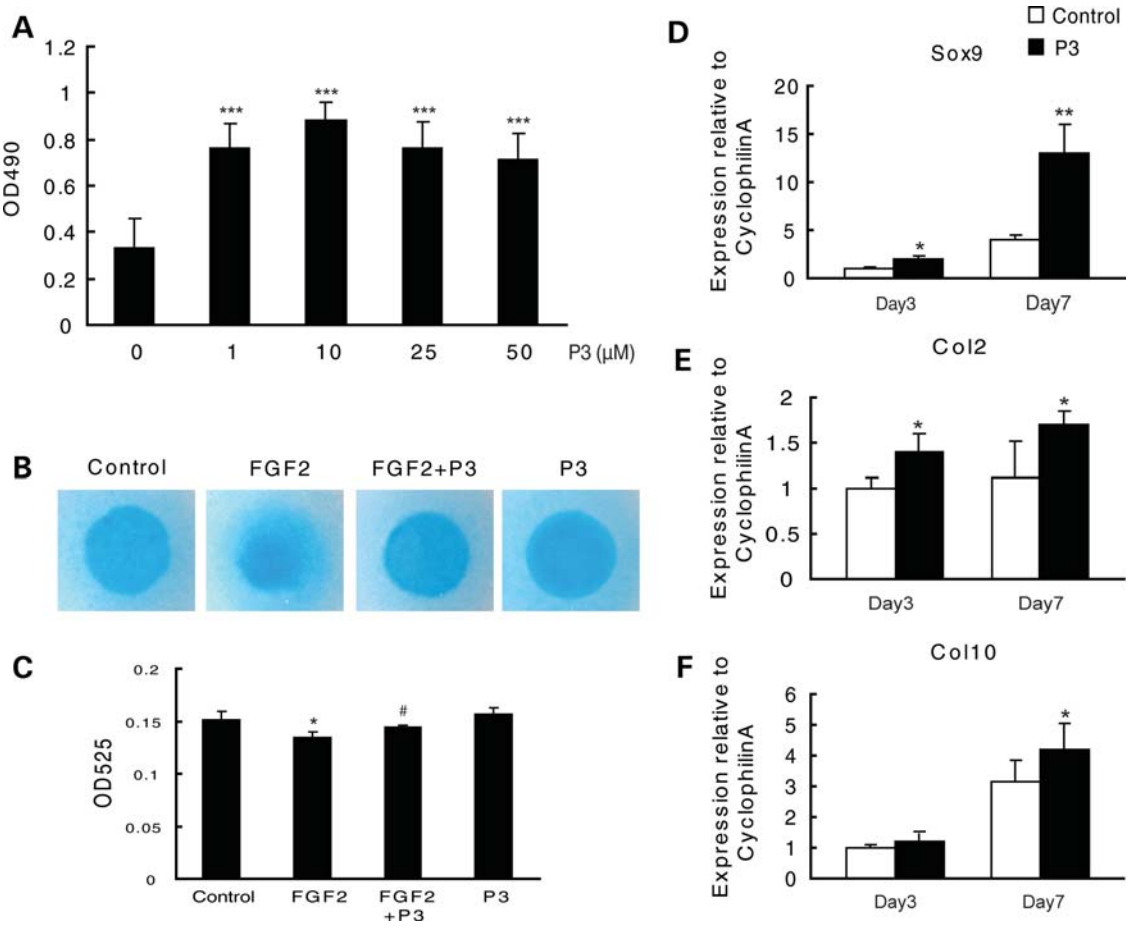

Figure 3. Peptide P3 promotes the proliferation and chondrogenic differentiation of ATDC5 cells. (**A**) MTT proliferation assay showing that P3 increases the proliferation of ATDC5 cells ($n = 6$, $^{***}P < 0.01$, versus control). (**B**) ATDC5 cells in micormass cultures were treated with FGF2 (20 ng/ml) and/or P3 (10 μM), and were stained with Alcian blue on Day 7. (**C**) DMMB assay for quantification of sulfated glycosaminoglycans in micormass culture ($n = 3$, $^{*}P < 0.05$, versus control. $^{\#}P < 0.05$, versus FGF2). (**D**–**F**) Relative mRNA expression levels of chondrogenic marker genes were measured by real-time PCR. The expression levels of *Sox9*, *Col2* and *Col10* mRNA in chondrogenic ATDC5 cells were significantly increased on Day 7 after induction in the presence of P3 (10 μM). ($n = 3$, $^{*}P < 0.05$, $^{**}P < 0.01$, versus control.)

Peptide P3 rescues the lethal phenotype and partially restores the structural distortion of growth plates in TDII mice

We previously found that TDII mice died within several hours after birth as a result of restricted respiration caused by retarded thoracic cage development (18). Here, we treated pregnant *Fgfr3*$^{\text{Neo-K644E/+}}$ mice that had been crossed with male heterozygous EIIa-Cre mice with P3 peritoneal injection daily (100 μg/kg body weight) at E16.5 until birth. All TDII pups without P3 treatment died within a few hours after birth and showed abnormalities as described previously (18), including a dome-shaped skull, decreased ossification in the spine, ribs and epiphyses and obvious curvature of the axial skeleton, whereas all TDII pups treated with peptide P3 were survived (Fig. 5A–D). Among the 104 mice born by pregnant mice injected with P3, 12 of them were TDII mice. All these mutant mice were survived after birth to maximal 140 days (Table 2, Fig. 5B and C). Although P3-treated TDII mice survived from early postnatal lethality, they still exhibited small habius, short and round skull (Fig. 5B and C). Examination of the cranial base revealed a premature closure of the spheno-occipital synchondroses in TDII mice, and the premature closure of the cranial bases of TDII mice treated with peptide P3 and WT mice appeared to be normal (Fig. 5E). Skeleton preparations of newborn pups showed that treatment with P3 reversed the abnormal ossification of sternebrae and the widening of the sternum and costal cartilage in TDII mice (Fig. 5F and G). Examination of the long bones revealed that treatment with P3 alleviated the shortening of long bones in TDII mice (Fig. 5H–K).

Histological examinations using H&E staining revealed a reduction in width of the hypertrophic zone of growth plates of the TDII mice with small hypertrophic chondrocytes compared with WT mice (Fig. 6A). When treated with peptide P3, the hypertrophic zone was markedly expanded and the morphology of the proliferative and hypertrophic chondrocytes significantly changed (Fig. 6A). The hypertrophic chondrocytes in the P3-treated growth plates appeared to be more spherical and enlarged, resembling to hypertrophic chondrocytes in the growth plates of WT mice. However, although the growth plates of the P3-treated TDII mice were remarkably improved, the width of the proliferative and hypertrophic

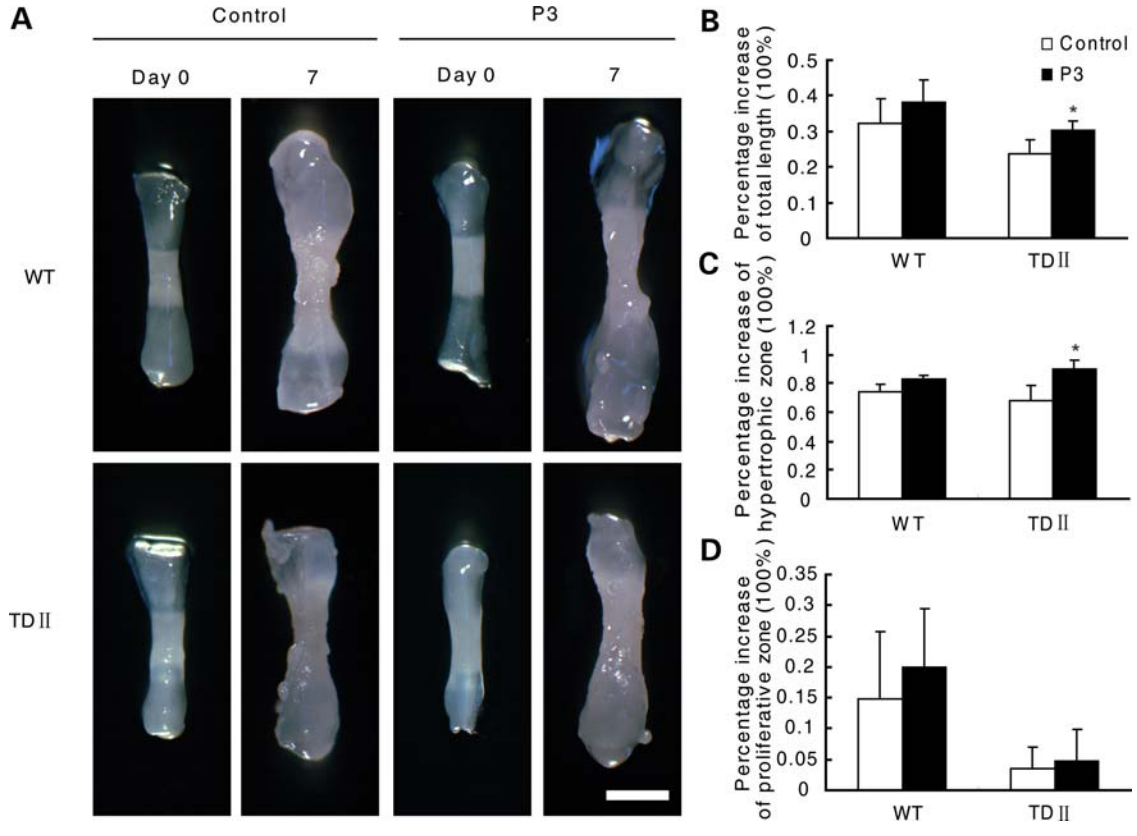

Figure 4. Peptide P3 suppresses FGFR3-mediated growth inhibition in cultured murine metatarsal bones. (**A**) Representative photographs show the rescuing effects of peptide P3 on growth retarded of cultured metatarsal bones from TDII mice. Scale bar, 500 μm. (**B**–**D**) Quantification of the percentage increases in total length, and the lengths of hypertrophic and proliferative zones of metatarsal bones from TDII or WT mice cultured for 7 days in the absence (control) or presence of P3 (10 μM). ($n = 4$, $^{*}P < 0.05$, versus control.)

zones was still reduced when compared with WT mice (Fig. 6A and B). Histological staining showed that the tibial trabecular bone of P3-treated TDII mouse at 140 days was sparser than that of WT mice, suggesting that the bone formation via endochondrol ossification was still impaired in P3-treated TDII mice (Fig. 6C, Supplementary Material, Fig. S2). These results demonstrate that treatment with P3 significantly rescued the severe defects of growth plate development in TDII mice by restoring the disrupted chondrocyte maturation process. Histological analysis of lung tissues of new born WT mice showed formation of large alveoli, while alveoli were not well formed in TDII mice as described previously (18). In contrast, the morphology of lung tissues in P3-treated TDII mice was similar to that in WT mice, which had grossly normal alveoli formation (Fig. 6D).

DISCUSSION

Activating FGFR3 mutations in humans are associated with several types of dwarfisms (2,4,19). Among them, ACH patients exhibit short stature especially in the proximal upper and lower limbs, central facial dysplasia, macrocephaly and spine protrusion (19–21). TD, the most common form of lethal skeletal dysplasia, is featured by macrocephaly, narrow bell-shaped thorax and severe shortening of the limbs, and lethality in the neonatal period (5,22).

At present, there are few approaches used to treat ACH/TD patients: mainly growth hormone therapy and surgical limb lengthening. However, treatment with growth hormone for ACH patients has no clear long-term benefit (23–25). Surgical limb lengthening can only increase the limb length to some extent and the procedure is controversial and highly invasive and may cause severe complications including fractures and infections (26,27). Moreover, the macrocephaly and spinal stenosis in ACH cannot be readily corrected by surgical intervention (28). Because of its neonatal lethality, it is extremely difficult to deliver surgical and growth hormone treatment to TD patients. Thus, more effective rationalized treatments are urgently needed for these skeletal disorders. Given its causal role in these skeletal disorders, FGFR3 and/or its downstream pathways are attractive targets for therapy. Indeed, C-natriuretic peptide (CNP) is a newly identified potential therapeutic antagonist of FGFR3 signaling that alleviates dwarfism phenotype of ACH mice through its inhibition on the FGFR3–MAPK pathway (29,30). In addition, we have found previously that parathyroid hormone (PTH)-related peptide (PTHrP) partially reversed the shortening of cultured bone rudiments from mice mimicking human ACH (31). Human PTH (1–34) stimulated the longitudinal bone growth in rats and improved the growth of the cultured femurs from mice expressing FGFR3 carrying a gain-of-function mutation (G380R) (32,33).

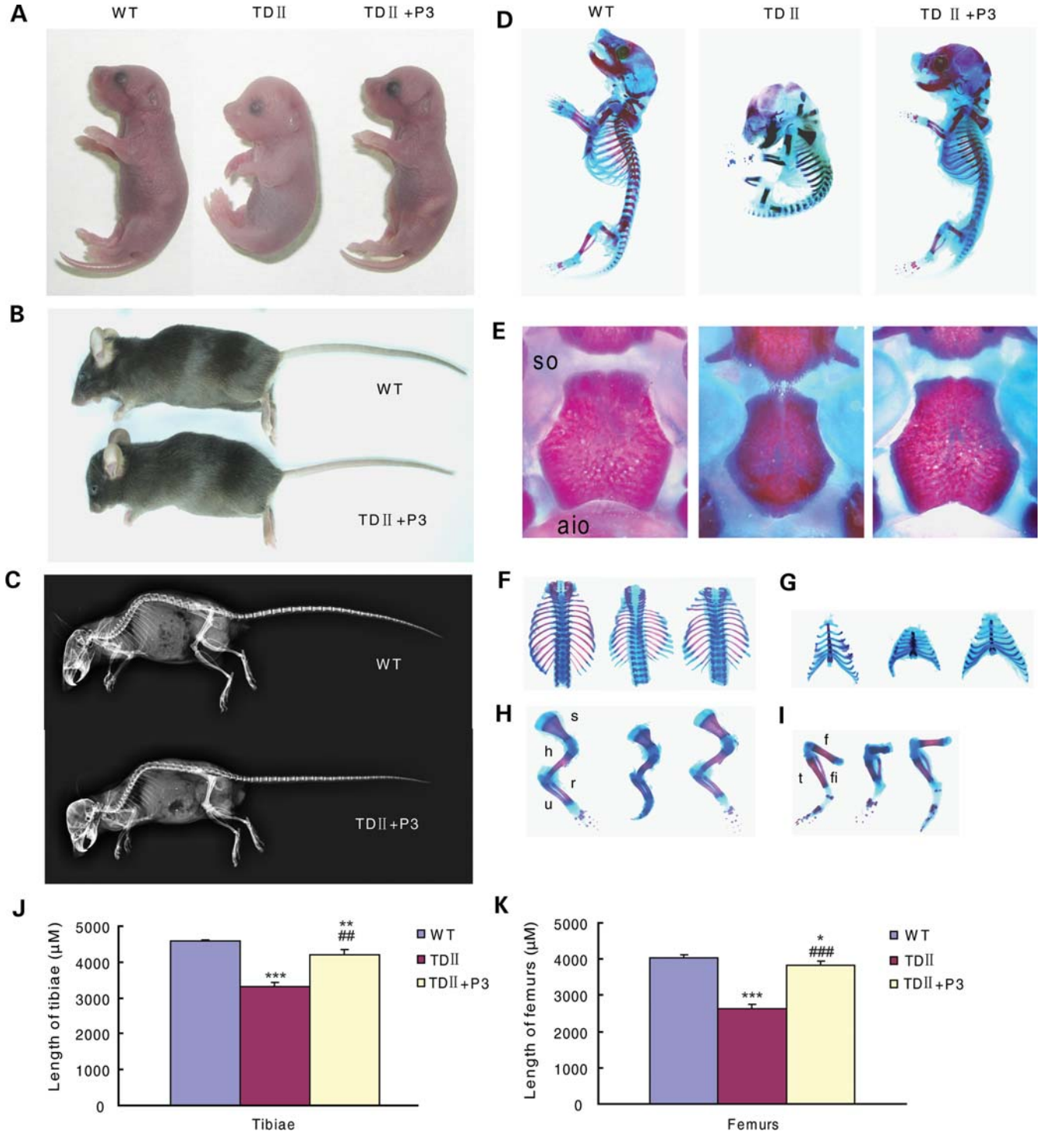

Figure 5. Peptide P3 rescues the lethal phenotype in thanatophoric dysplasia type II (TDII) mice. (**A**) WT mice and TDII mice treated with or without peptide P3 at P1. (**B**) TDII mouse treated with peptide P3 and the WT controls at P140. (**C**) X-ray images of the TDII mouse treated with peptide P3 and the WT controls at P140. (**D**) Alizarin red and Alcain blue staining of the skeletons of WT and TDII mice treated with or without peptide P3 at P1. (**E**) Cranial base stained with Alizarin red and Alcain blue in WT and TDII mice treated with or without peptide P3 at P1. (**F**–**I**) Thoracic cages (F), forelimbs (H) and hindlimbs (I) of WT, TDII and P3-treated mice at P1. (**J** and **K**) Quantification of tibial and femoral length of WT mice, TDII mice and P3-treated mice at P1. ($n = 3$, $^{*}P < 0.05$, $^{**}P < 0.01$, $^{***}P < 0.001$, versus WT. $^{\#\#}P < 0.01$, $^{\#\#\#}P < 0.001$, versus TDII.) so, spheno-occipital; aio, anterior intraoccipital; s, scapula; h, humerus; r, radius; u, ulna; f, femur; t, tibia; fi, fibula.

Table 2. Summary of survival of TDII mice[a] with P3 treatment

ID	Sex	Phenotypes (after treatment)
1	M	Died at 32 days
2	M	Died at 51 days
3	F	Died at 54 days
4	M	Died at 59 days
5	M	Died at 60 days
6–7	M	Died at 64 days
8–9	M,F	Died at 78 days
10–11	M	Died at 120 days
12	M	Died at 140 days

[a]All these mice received the treatment with peptide P3 (100 μgkg body weight per day) during gestation from E16.5 to newborn via intraperitoneal injection.

Different approaches have been used to block the signaling of transmembrane receptors, including chemicals, neutralizing antibody and peptides (15,34). Among them, peptides are getting more attention in drug development for their advantages (35,36). In addition, peptides can easily be synthesized and purified (37), and peptide drugs have successfully been used in clinics such as α1-thymosin (38). The efficient phage display technique has widely been used in screening the candidate peptide drugs (39,40).

In the present study, we have screened a random 12-peptide phage library to identify FGFR3 antagonists, from which 44 phage clones had been identified to selectively bind to FGFR3 and 23 of these clones have identical sequence. Furthermore, we have shown that this peptide (P3) specifically binds the extracellular domain of FGFR3 with a high affinity, suggesting the specific effect of P3 on FGFR3 activity. Indeed, we have found that peptide P3 inhibits activation of WT FGFR3 or constitutively active mutant FGFR3 (K650M and K664E). We further have proved that P3 markedly decreases the FGF2-induced ERK1/2 phosphorylation in FGFR3-expressing ATDC5 chondrogenic cells, suggesting the ability of P3 in inhibition of the ERK/MAPK pathway of FGFR3 signaling.

The growth retardation of long bones in ACH and TD patients or mice is caused by reduced chondrocyte proliferation and differentiation, as well as increased chondrocyte apoptosis (41–43). In this study, we have shown that P3 suppresses the tyrosine kinase activity of FGFR3 and FGFR3-mediated ERK/MAPK activation, which is speculated to be the molecular basis for the rescuing effect of P3 on the retarded chondrocyte development, in bone rudiments cultures using the long bone derived from the mice mimicking human TDII. Consistently, inhibition of the ERK/MAPK pathway by CNP or U0126 was also found to alleviate the skeletal phenotypes of mice mimicking human ACH or Apert syndrome resulting from gain-of-function mutation in FGFR3 or FGFR2, respectively (29,34). These findings are supportive for our P3 rescuing experiments.

TDII patients usually die early after birth because of respiratory failure. In this study, we treated pregnant *Fgfr3*$^{Neo\text{-}K644E/+}$ mice that had been crossed with male heterozygous EIIa-Cre mice with daily intraperitoneal injection of P3 at E16.5 until birth. Among the 104 mice born by pregnant mice injected with P3, 12 of them were TDII mice. The reason for the low yield of TDII mice is currently unclear. Although we cannot exclude the potential side effects of P3, we suspect that the combined effect of differences in environment, generation and genetic background might contribute to this difference. More importantly, we found that P3-treated TDII mice developed a relatively normal thoracic cavity and lung structure compared with that of WT mice, which further supports the notion that the respiratory distress in TD patients is due to defects in cartilage/bone development of thoracic cavity. No gross histopathologic difference was found in other important organs, such as the heart, liver, spleen and kidney in TDII and WT mice born by pregnant mice treated with P3 (data not shown). Down-regulation of FGFR3 activity in humans and knockout of the *Fgfr3* gene in mice cause mainly bone overgrowth, and no significant abnormalities have been reported (6,44,45). Given the ethical issues raised by treating TD patients, P3 may more practically be used to treat ACH patients, one of the most common forms of dwarfism.

Although this novel peptide has been found to rescue the bone growth retardation and postnatal lethality phenotype of mice mimicking human TDII, we noticed that the rescued TDII mice still had smaller body size than WT littermates, and the skull of the P3-treated TDII mice were still dome-shaped. Thus, further studies are required to optimize the structure of the peptide and formulations (dosage, timing, length of treatment, delivery, and/or combined application with other measures such as growth hormone and PTH), which may further improve the treatment outcome on skeletal phenotype.

Taken together, a novel peptide that binds to and antagonizes FGFR3 activity has been obtained by phage display approach. This peptide promotes chondrocyte proliferation and differentiation and subsequently rescues bone growth retardation and postnatal lethality phenotype of mice mimicking human TDII. This peptide may serve as a novel candidate peptide for the treatment of FGFR3-related skeletal dysplasia. In addition, since somatic gain-of-function mutations of FGFR3 have been found to be involved in bladder cancer, multiple myeloma and cervical cancer (46–53), this peptide may also serve as a novel inhibitor of FGFR3-signaling activity in cancer treatment.

MATERIALS AND METHODS

Biopanning of a 12-peptide phage display library with FGFR3

The PhD^{TM} phage display peptide library (New England Biolabs) was used for biopanning. Microtiter plates (96-well) were coated with 20 μg/ml FGFR3 (Sigma) overnight at 4°C and then were blocked with 1% (wt/vol) bovine serum albumin (BSA, Sigma) for 1 h at 37°C. The plates were washed six times (1 min each) with 0.05% Tween-20 in phosphate-buffered saline (PBS). Sequentially, the PhD^{TM} peptide library was added and shaken gently at room temperature for 1 h. After the plates were washed 10 times (1 min each) with 0.05% Tween-20 in PBS, each well of the plates was eluted with Gly-HCl buffer (pH 2.2) and neutralized with 1 M Tris–HCl (pH 9.1). Then the titer of the phage elution was detected. The eluate was amplified and purified

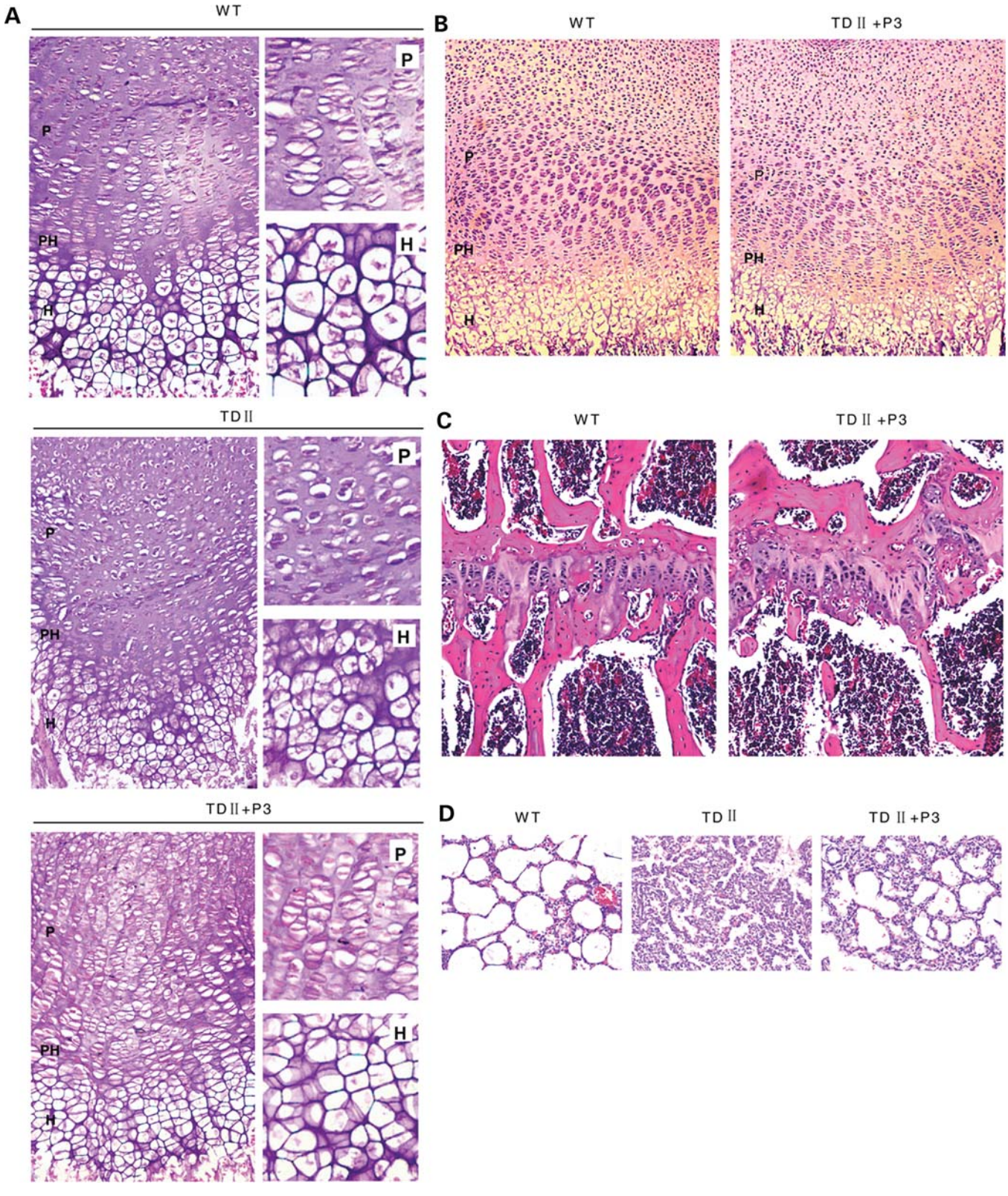

Figure 6. Peptide P3 rescues the abnormal growth plate and the lung phenotypes in the TDII mice. (**A**) Histology of the growth plate of proximal tibia in WT, TDII and P3-treated mice at P1. (**B** and **C**) Histological analysis of proximal tibia in WT and P3-treated mice at P5 (B) and P140 (C). (**D**) Morphology of the lungs in WT, TDII and P3-treated mice at P1.

for the next round of selection. Two additional rounds of screening were performed under conditions as follows: the amount of FGFR3 coated in the plates was reduced (1.5 μg/ml in the second round of screening, 1 μg/ml in the third round). Moreover, the concentration of Tween-20 in PBS used for washing was increased (0.1% for the second round and 0.2% for the third round) and the time for washing was longer (10 × 2 min for the second round and 10 × 3 min for the third round).

ELISA assay for selected phage clones

Microtiter plates were coated with FGFR3 (20 μg/ml) and blocked with 1% BSA as above. Then the plates were washed six times (5 min each) with 0.05% Tween-20 in PBS. Phage clones (2×10^{11} pfu/well) and control phage vcsM13 were added and incubated at room temperature for 1 h. For competitive elution, FGF2 (2 μg/ml) was added for incubation at room temperature for 1 h. After the plates were washed six times (5 min each) with 0.05% Tween-20 in PBS, anti-M13 antibody (Amersham Pharmacia) was added and incubated at 37°C for 1 h. The plates were washed six times with 0.05% Tween-20 in PBS. Next goat anti-mouse immunoglobulin G (IgG)–HRP was added and incubated at 37°C for 30 min. The plates were washed again with 0.05% Tween-20 in PBS and color development was initiated with addition of 3,3′,5,5′-tetramethylbenzidine (TMB; 100 μl/well of TMB). The reaction was terminated 20 min later by adding 20 μl stopping buffer, and the absorbance was measured at 450 nm.

Isolation and sequencing of phage DNA and peptide synthesis

Total DNA of individual phage clones was isolated according to the sequencing kit manufacturer's recommended protocol (Biosystems). The isolated DNA of the positive clones was sequenced using an automated DNA sequencer at Shanghai Sangon Company. DNA sequences were analyzed using the BioEdit Sequence Alignment Editor software and the ProtParam programs. The peptides were synthesized at Shanghai ChinaPeptides Co., Ltd. by solid-phase synthesis and purified by high-performance liquid chromatography (HPLC).

Peptide P3 and FGFR3-binding assays

Ninety-six-well microtiter plates were coated with 100 μl of increasing amount of P3 overnight at 4°C. After blocking with 5% BSA at 37°C for 1 h, 150 μl of 20 μg/ml of either the extracellular region of FGFR3 (Sigma) or the intracellular region of FGFR3 (GST-fused FGFR3-ICD expressed in *Escherichia coli* strain BL21 cells and purified by affinity chromatography with glutathione–Sepharose 4B resin) (GE Healthcare) was added and incubated at 37°C for 1 h. Plates were washed and incubated with biotinylated extracellular domain of FGFR3 antibody (Sigma) or biotinylated intracellular domain of FGFR3 antibody (Santa Cruz Biotechnology), followed by a secondary antibody conjugated with HRP (DAKO), and 5-amino-2-hydroxybenzoic acid as a substrate, with absorbance measured at 450 nm in an ELISA Reader.

Cell culture and cell viability assay

Mouse embryonic carcinoma-derived cell line ATDC5 cells were cultured in 96-well plates (1×10^4 cells/well) in Dulbecco's Modified Eagle Medium (DMEM)/F12 (1:1) media, supplemented with 5% fetal bovine serum (FBS) and incubated for 24 h. The cells were washed with DMEM/F12 and cultured in DMEM/F12 containing no FBS to starve the cells overnight. The medium was then replaced by DMEM/F12 containing serially diluted P3 alone. After being cultured for 24 h, the number of viable cells was determined by the MTT method as described previously (54).

In vitro chongdrogenesis assay

Cells were plated at 1×10^5 cells/35 mm well in DMEM/F12 (1:1) containing 5% FBS. The cells were grown for 3 days after which the medium in the absence or presence of 10 μM of P3 was supplemented with 10 μg/ml human transferrin (Sigma), 3×10^{-8}M sodium selenite (Sigma), 10 μg/ml bovine insulin (Sigma) to induce chondrogenesis for 7 days (55). The medium was replaced every other day. The cells were harvested at Day 3 and 7 of chondrogenic induction.

Micromass culture

ATDC5 cells were cultured in micromass cultures as described previously (56). Briefly, ATDC5 cells were suspended in DMEM/F-12 (1:1) medium containing 5% FBS, 10 mg/ml streptomycin, 10 U/ml penicillin at a density of 1×10^7 cells/ml and plated in 10 μl droplets to simulate the high density chondrogenic condensations. After plating for 1 h, medium (as above, supplemented with 10 μg/ml human transferrin, 3×10^{-8} M sodium selenite, 10 μg/ml bovine insulin) was added to the cultures and supplemented with 20 ng/ml of FGF2, 10 μM P3 or 20 ng/ml of FGF2 together with 10 μM P3. Medium were changed every 24 h until harvesting.

DMMB assay

DMMB dye solution and sample digestion solution were prepared as described previously (57). Each sample at 100 μl and 2.5 ml DMMB dye solution were mixed and poured into aspectrophotometer cuvette, and the absorbance was measured at 525 nm immediately.

Mice

Fgfr3$^{Neo\text{-}K644E/+}$ mice were generated by us before (18). *Fgfr3*$^{Neo\text{-}K644E/+}$ mice were crossed with heterozygous EIIa-Cre mice (58) to obtain *Fgfr3*$^{Neo\text{-}K644E/+}$ EIIa-Cre mice (TDII mice). All experiments were performed in accordance with the protocols approved by the Institutional Animal Care and Use Committee of Daping Hospital.

Bone explant culture

Metatarsal rudiments were isolated from WT and TDII mouse fetuses at E19.5. Metatarsals were dissected out under the microscope and cultured in 48-well plates with BGJb

medium supplemented with 0.05 mg/ml ascorbic acid, 0.5 mg/ml L-glutamine, 10 mg/ml streptomycin, 10 U/ml penicillin, 1 mM β-glycerophosphate and 0.2% BSA. Metatasals were further treated with peptide P3 at 10 μM for 7 days. Medium was changed on the second day of culture. The rudiments were observed and photographed under a dissecting microscope (Leica) at 0 and 7 days of treatment. Two sets of pictures were taken under different light direction (light from the top of samples or from the bottom). The TL was measured with an eyepiece scale. The lengths of hypertrophic and proliferative zones were measured approximately as described previously (31). The length of hypertrophic zone includes the regions of both the mineralized (the dark area) and unmineralized (the light non-mineralizing areas flanking the dark area) hypertrophic chondrocytes. The length of proliferative zone is calculated as the difference between the total length and the hypertrophic length. Changes in length were expressed as percentage increase relative to the value before the treatment (percentage increase = [length at Day 7 – length at Day 0]/length at Day 0).

Real-time PCR

From treated ATDC5 cells, total RNA was isolated by TRIZOL reagent (Invitrogen). Real-time PCR was repeated at least three times using Max3000 PCR machine (Stratagene) and SYBR Premix Ex TaqTM kit (Takara). Expression values were normalized to Cyclophilin A. The primer sequences were as follows: *Sox9*, 5′-TTCCTCCTCCCGGCATGAGTG-3′ and 5′-CAACTTTGCCAGCTTGCACG-3′. *Col2*, 5′-CTGGTGGAGCAGCAAGAGCAA-3′ and 5′-CAGTGGACAGTAGACGGAGGAAAG-3′; *Col10*, 5′-GCAGCATTACGACCCAAGAT-3′ and 5′-CATGATTGCACTCCCTGAAG-3′; *Cyclophilin A*, 5′-CGAGCTCTGAGCACTGGAGA-3′ and 5′-TGGCGTGTAAAGTCACCACC-3′.

In vitro activation of FGFR3

HEK293T cells were plated in 60 mm dishes the day before transfection. Five micrograms of WT, K650M mutant and K644E mutant of FGFR3 constructs (pRK7/M2-huFGFR3-WT, pRK7/M2-huFGFR3-K650M, pcDNA3.1/Myc-muFGFR3-K644E) were transfected individually. After transfection for 24 h, cells were incubated for 6 h in the absence or presence of 10 μM P3. Cells were lysed, immunoprecipitated with anti-M2 antibody (Sigma) or anti-Myc antibody (Santa Cruz Biotechnology). Blots were developed using anti-phospho-tyrosine antibody (Millipore). Lysates were analyzed by immunoblotting with antibodies against FGFR3 (Santa Cruz Biotechnology) and β-actin (Sigma) as controls.

Western blot analysis

ATDC5 cells were lysed in an ice-cold buffer containing 50 mM Tris–HCl (pH 7.4), 150 mM NaCl, 1% Nonidet P-40, 0.1% sodium dodecyl sulfate (SDS), and a cocktail of protease inhibitors (Roche). Protein samples (10 μg) were resolved on a 10% SDS- polyacrylamide gel electrophoresis (PAGE) gel and transferred onto a polyvinylidene difluoride membrane (Millipore). Then antibodies against phospho-ERK1/2 (Cell Signaling) and β-actin (Sigma) were used to probe the blots followed by enhanced chemiluminescent signal detection.

Skeletal analysis and histology

The whole-skeleton staining with Alizarin red and Alcian blue was performed as described by McLeod (59). Whole skeletons were harvested, stored in 70% ethanol and were subjected to high-resolution X-ray examination. For histological analysis, the tibiae were fixed in 4% paraformaldehyde in 0.01 M PBS (pH 7.4), decalcified in 15% ethylenediamminetetraacetate (pH 7.4) and embedded in paraffin as previously described (54). Sections (6 μm) were stained with Hematoxylin and Eosin (H&E).

Statistical analysis

Data were presented as mean OD values ± SD and statistical differences between groups were assessed by Student's *t*-test, assuming double-sided independent variance and *P*-values of <0.05 were considered significant.

SUPPLEMENTARY MATERIAL

Supplementary material is available at *HMG* online.

ACKNOWLEDGEMENTS

We thank Dr Westphal (National Institutes of Health, USA) for providing EIIa-Cre mice and Jing Yang and Siyu Chen (Daping Hospital, Third Military Medical University, Chongqing, China) for technical support.

Conflict of Interest statement. None declared.

FUNDING

The work was supported by National Natural Science Foundation of China (No.81001390, No.81030036, No. 30971607, No.81170809, No.SKLZZ201017), the Special Funds for Major State Basic Research Program of China (973 Program) (No.2012CB518106, No.2011CB964701).

REFERENCES

1. Xian, C.J. (2007) Roles of epidermal growth factor family in the regulation of postnatal somatic growth. *Endocr. Rev.*, **28**, 284–296.
2. Shiang, R., Thompson, L.M., Zhu, Y.Z., Church, D.M., Fielder, T.J., Bocian, M., Winokur, S.T. and Wasmuth, J.J. (1994) Mutations in the transmembrane domain of FGFR3 cause the most common genetic form of dwarfism, achondroplasia. *Cell*, **78**, 335–342.
3. Horton, W.A. (1997) Fibroblast growth factor receptor 3 and the human chondrodysplasias. *Curr. Opin. Pediatr.*, **9**, 437–442.
4. Bonaventure, J., Rousseau, F., Legeai-Mallet, L., Le Merrer, M., Munnich, A. and Maroteaux, P. (1996) Common mutations in the fibroblast growth factor receptor 3 (FGFR 3) gene account for achondroplasia, hypochondroplasia, and thanatophoric dwarfism. *Am. J. Med. Genet.*, **63**, 148–154.
5. Rousseau, F., el Ghouzzi, V., Delezoide, A.L., Legeai-Mallet, L., Le Merrer, M., Munnich, A. and Bonaventure, J. (1996) Missense FGFR3 mutations create cysteine residues in thanatophoric dwarfism type I (TD1). *Hum. Mol. Genet.*, **5**, 509–512.

6. Toydemir, R.M., Brassington, A.E., Bayrak-Toydemir, P., Krakowiak, P.A., Jorde, L.B., Whitby, F.G., Longo, N., Viskochil, D.H., Carey, J.C. and Bamshad, M.J. (2006) A novel mutation in FGFR3 causes camptodactyly, tall stature, and hearing loss (CATSHL) syndrome. *Am. J. Hum. Genet.*, **79**, 935–941.
7. Naski, M.C., Colvin, J.S., Coffin, J.D. and Ornitz, D.M. (1998) Repression of hedgehog signaling and BMP4 expression in growth plate cartilage by fibroblast growth factor receptor 3. *Development*, **125**, 4977–4988.
8. Chen, L., Adar, R., Yang, X., Monsonego, E.O., Li, C., Hauschka, P.V., Yayon, A. and Deng, C.X. (1999) Gly369Cys mutation in mouse FGFR3 causes achondroplasia by affecting both chondrogenesis and osteogenesis. *J. Clin. Invest.*, **104**, 1517–1525.
9. Ornitz, D.M. and Marie, P.J. (2002) FGF signaling pathways in endochondral and intramembranous bone development and human genetic disease. *Genes. Dev.*, **16**, 1446–1465.
10. Li, C., Chen, L., Iwata, T., Kitagawa, M., Fu, X.Y. and Deng, C.X. (1999) A Lys644Glu substitution in fibroblast growth factor receptor 3 (FGFR3) causes dwarfism in mice by activation of STATs and ink4 cell cycle inhibitors. *Hum. Mol. Genet.*, **8**, 35–44.
11. Su, W.C., Kitagawa, M., Xue, N., Xie, B., Garofalo, S., Cho, J., Deng, C., Horton, W.A. and Fu, X.Y. (1997) Activation of Stat1 by mutant fibroblast growth-factor receptor in thanatophoric dysplasia type II dwarfism. *Nature*, **386**, 288–292.
12. Sahni, M., Ambrosetti, D.C., Mansukhani, A., Gertner, R., Levy, D. and Basilico, C. (1999) FGF signaling inhibits chondrocyte proliferation and regulates bone development through the STAT-1 pathway. *Genes. Dev.*, **13**, 1361–1366.
13. Murakami, S., Balmes, G., McKinney, S., Zhang, Z., Givol, D. and de Crombrugghe, B. (2004) Constitutive activation of MEK1 in chondrocytes causes Stat1-independent achondroplasia-like dwarfism and rescues the Fgfr3-deficient mouse phenotype. *Genes. Dev.*, **18**, 290–305.
14. Ornitz, D.M. (2000) FGFs, heparan sulfate and FGFRs: complex interactions essential for development. *Bioessays*, **22**, 108–112.
15. Qing, J., Du, X., Chen, Y., Chan, P., Li, H., Wu, P., Marsters, S., Stawicki, S., Tien, J., Totpal, K. *et al.* (2009) Antibody-based targeting of FGFR3 in bladder carcinoma and t(4;14)-positive multiple myeloma in mice. *J. Clin. Invest.*, **119**, 1216–1229.
16. Shimizu, A., Tada, K., Shukunami, C., Hiraki, Y., Kurokawa, T., Magane, N. and Kurokawa-Seo, M. (2001) A novel alternatively spliced fibroblast growth factor receptor 3 isoform lacking the acid box domain is expressed during chondrogenic differentiation of ATDC5 cells. *J. Biol. Chem.*, **276**, 11031–11040.
17. Altaf, F.M., Hering, T.M., Kazmi, N.H., Yoo, J.U. and Johnstone, B. (2006) Ascorbate-enhanced chondrogenesis of ATDC5 cells. *Eur. Cell Mater.*, **12**, 64–69; discussion 69–70.
18. Iwata, T., Chen, L., Li, C., Ovchinnikov, D.A., Behringer, R.R., Francomano, C.A. and Deng, C.X. (2000) A neonatal lethal mutation in FGFR3 uncouples proliferation and differentiation of growth plate chondrocytes in embryos. *Hum. Mol. Genet.*, **9**, 1603–1613.
19. Rousseau, F., Bonaventure, J., Legeai-Mallet, L., Pelet, A., Rozet, J.M., Maroteaux, P., Le Merrer, M. and Munnich, A. (1994) Mutations in the gene encoding fibroblast growth factor receptor-3 in achondroplasia. *Nature*, **371**, 252–254.
20. Bellus, G.A., Hefferon, T.W., Ortiz de Luna, R.I., Hecht, J.T., Horton, W.A., Machado, M., Kaitila, I., McIntosh, I. and Francomano, C.A. (1995) Achondroplasia is defined by recurrent G380R mutations of FGFR3. *Am. J. Hum. Genet.*, **56**, 368–373.
21. Passos-Bueno, M.R., Wilcox, W.R., Jabs, E.W., Sertie, A.L., Alonso, L.G. and Kitoh, H. (1999) Clinical spectrum of fibroblast growth factor receptor mutations. *Hum. Mutat.*, **14**, 115–125.
22. Tavormina, P.L., Shiang, R., Thompson, L.M., Zhu, Y.Z., Wilkin, D.J., Lachman, R.S., Wilcox, W.R., Rimoin, D.L., Cohn, D.H. and Wasmuth, J.J. (1995) Thanatophoric dysplasia (types I and II) caused by distinct mutations in fibroblast growth factor receptor 3. *Nat. Genet.*, **9**, 321–328.
23. Shohat, M., Tick, D., Barakat, S., Bu, X., Melmed, S. and Rimoin, D.L. (1996) Short-term recombinant human growth hormone treatment increases growth rate in achondroplasia. *J. Clin. Endocrinol. Metab.*, **81**, 4033–4037.
24. Stamoyannou, L., Karachaliou, F., Neou, P., Papataxiarchou, K., Pistevos, G. and Bartsocas, C.S. (1997) Growth and growth hormone therapy in children with achondroplasia: a two-year experience. *Am. J. Med. Genet.*, **72**, 71–76.
25. Weber, G., Prinster, C., Meneghel, M., Russo, F., Mora, S., Puzzovio, M., Del Maschio, M. and Chiumello, G. (1996) Human growth hormone treatment in prepubertal children with achondroplasia. *Am. J. Med. Genet.*, **61**, 396–400.
26. Aldegheri, R. and Dall'Oca, C. (2001) Limb lengthening in short stature patients. *J. Pediatr. Orthop. B*, **10**, 238–247.
27. Aldegheri, R., Trivella, G., Renzi-Brivio, L., Tessari, G., Agostini, S. and Lavini, F. (1988) Lengthening of the lower limbs in achondroplastic patients. A comparative study of four techniques. *J. Bone Joint Surg. Br.*, **70**, 69–73.
28. Aviezer, D., Golembo, M. and Yayon, A. (2003) Fibroblast growth factor receptor-3 as a therapeutic target for Achondroplasia—genetic short limbed dwarfism. *Curr. Drug Targets*, **4**, 353–365.
29. Yasoda, A., Komatsu, Y., Chusho, H., Miyazawa, T., Ozasa, A., Miura, M., Kurihara, T., Rogi, T., Tanaka, S., Suda, M. *et al.* (2004) Overexpression of CNP in chondrocytes rescues achondroplasia through a MAPK-dependent pathway. *Nat. Med.*, **10**, 80–86.
30. Ozasa, A., Komatsu, Y., Yasoda, A., Miura, M., Sakuma, Y., Nakatsuru, Y., Arai, H., Itoh, N. and Nakao, K. (2005) Complementary antagonistic actions between C-type natriuretic peptide and the MAPK pathway through FGFR-3 in ATDC5 cells. *Bone*, **36**, 1056–1064.
31. Chen, L., Li, C., Qiao, W., Xu, X. and Deng, C. (2001) A Ser(365)–>Cys mutation of fibroblast growth factor receptor 3 in mouse downregulates Ihh/PTHrP signals and causes severe achondroplasia. *Hum. Mol. Genet.*, **10**, 457–465.
32. Ogawa, T., Yamagiwa, H., Hayami, T., Liu, Z., Huang, K.Y., Tokunaga, K., Murai, T. and Endo, N. (2002) Human PTH (1–34) induces longitudinal bone growth in rats. *J. Bone Miner. Metab.*, **20**, 83–90.
33. Ueda, K., Yamanaka, Y., Harada, D., Yamagami, E., Tanaka, H. and Seino, Y. (2007) PTH has the potential to rescue disturbed bone growth in achondroplasia. *Bone*, **41**, 13–18.
34. Shukla, V., Coumoul, X., Wang, R.H., Kim, H.S. and Deng, C.X. (2007) RNA interference and inhibition of MEK-ERK signaling prevent abnormal skeletal phenotypes in a mouse model of craniosynostosis. *Nat. Genet.*, **39**, 1145–1150.
35. Hamman, J.H., Enslin, G.M. and Kotze, A.F. (2005) Oral delivery of peptide drugs: barriers and developments. *BioDrugs*, **19**, 165–177.
36. Gomez-Orellana, I. (2005) Strategies to improve oral drug bioavailability. *Expert Opin. Drug Deliv.*, **2**, 419–433.
37. Joshi, M.B., Gam, A.A., Boykins, R.A., Kumar, S., Sacci, J., Hoffman, S.L., Nakhasi, H.L. and Kenney, R.T. (2001) Immunogenicity of well-characterized synthetic *Plasmodium falciparum* multiple antigen peptide conjugates. *Infect. Immun.*, **69**, 4884–4890.
38. Chien, R.N., Liaw, Y.F., Chen, T.C., Yeh, C.T. and Sheen, I.S. (1998) Efficacy of thymosin alpha1 in patients with chronic hepatitis B: a randomized, controlled trial. *Hepatology*, **27**, 1383–1387.
39. Barry, M.A., Dower, W.J. and Johnston, S.A. (1996) Toward cell-targeting gene therapy vectors: selection of cell-binding peptides from random peptide-presenting phage libraries. *Nat. Med.*, **2**, 299–305.
40. Scott, J.K. and Smith, G.P. (1990) Searching for peptide ligands with an epitope library. *Science*, **249**, 386–390.
41. Legeai-Mallet, L., Benoist-Lasselin, C., Delezoide, A.L., Munnich, A. and Bonaventure, J. (1998) Fibroblast growth factor receptor 3 mutations promote apoptosis but do not alter chondrocyte proliferation in thanatophoric dysplasia. *J. Biol. Chem.*, **273**, 13007–13014.
42. L'Hote, C.G. and Knowles, M.A. (2005) Cell responses to FGFR3 signalling: growth, differentiation and apoptosis. *Exp. Cell Res.*, **304**, 417–431.
43. Su, N., Du, X. and Chen, L. (2008) FGF signaling: its role in bone development and human skeleton diseases. *Front. Biosci.*, **13**, 2842–2865.
44. Deng, C., Wynshaw-Boris, A., Zhou, F., Kuo, A. and Leder, P. (1996) Fibroblast growth factor receptor 3 is a negative regulator of bone growth. *Cell*, **84**, 911–921.
45. Colvin, J.S., Bohne, B.A., Harding, G.W., McEwen, D.G. and Ornitz, D.M. (1996) Skeletal overgrowth and deafness in mice lacking fibroblast growth factor receptor 3. *Nat. Genet.*, **12**, 390–397.
46. Chesi, M., Nardini, E., Brents, L.A., Schrock, E., Ried, T., Kuehl, W.M. and Bergsagel, P.L. (1997) Frequent translocation t(4;14)(p16.3;q32.3) in multiple myeloma is associated with increased expression and activating mutations of fibroblast growth factor receptor 3. *Nat. Genet.*, **16**, 260–264.

47. Intini, D., Baldini, L., Fabris, S., Lombardi, L., Ciceri, G., Maiolo, A.T. and Neri, A. (2001) Analysis of FGFR3 gene mutations in multiple myeloma patients with t(4;14). *Br. J. Haematol.*, **114**, 362–364.
48. Cappellen, D., De Oliveira, C., Ricol, D., de Medina, S., Bourdin, J., Sastre-Garau, X., Chopin, D., Thiery, J.P. and Radvanyi, F. (1999) Frequent activating mutations of FGFR3 in human bladder and cervix carcinomas. *Nat. Genet.*, **23**, 18–20.
49. Hernandez, S., de Muga, S., Agell, L., Juanpere, N., Esgueva, R., Lorente, J.A., Mojal, S., Serrano, S. and Lloreta, J. (2009) FGFR3 mutations in prostate cancer: association with low-grade tumors. *Mod. Pathol.*, **22**, 848–856.
50. Muenke, M., Gripp, K.W., McDonald-McGinn, D.M., Gaudenz, K., Whitaker, L.A., Bartlett, S.P., Markowitz, R.I., Robin, N.H., Nwokoro, N., Mulvihill, J.J. *et al.* (1997) A unique point mutation in the fibroblast growth factor receptor 3 gene (FGFR3) defines a new craniosynostosis syndrome. *Am. J. Hum. Genet.*, **60**, 555–564.
51. Hafner, C., van Oers, J.M., Vogt, T., Landthaler, M., Stoehr, R., Blaszyk, H., Hofstaedter, F., Zwarthoff, E.C. and Hartmann, A. (2006) Mosaicism of activating FGFR3 mutations in human skin causes epidermal nevi. *J. Clin. Invest.*, **116**, 2201–2207.
52. Hafner, C., Stoehr, R., van Oers, J.M., Zwarthoff, E.C., Hofstaedter, F., Landthaler, M., Hartmann, A. and Vogt, T. (2009) FGFR3 and PIK3CA mutations are involved in the molecular pathogenesis of solar lentigo. *Br. J. Dermatol.*, **160**, 546–551.
53. Goriely, A., Hansen, R.M., Taylor, I.B., Olesen, I.A., Jacobsen, G.K., McGowan, S.J., Pfeifer, S.P., McVean, G.A., Rajpert-De Meyts, E. and Wilkie, A.O. (2009) Activating mutations in FGFR3 and HRAS reveal a shared genetic origin for congenital disorders and testicular tumors. *Nat. Genet.*, **41**, 1247–1252.
54. Su, N., Sun, Q., Li, C., Lu, X., Qi, H., Chen, S., Yang, J., Du, X., Zhao, L., He, Q. *et al.* (2010) Gain-of-function mutation in FGFR3 in mice leads to decreased bone mass by affecting both osteoblastogenesis and osteoclastogenesis. *Hum. Mol. Genet.*, **19**, 1199–1210.
55. Shukunami, C., Shigeno, C., Atsumi, T., Ishizeki, K., Suzuki, F. and Hiraki, Y. (1996) Chondrogenic differentiation of clonal mouse embryonic cell line ATDC5 *in vitro*: differentiation-dependent gene expression of parathyroid hormone (PTH)/PTH-related peptide receptor. *J. Cell Biol.*, **133**, 457–468.
56. Hoogendam, J., Parlevliet, E., Miclea, R., Lowik, C.W., Wit, J.M. and Karperien, M. (2006) Novel early target genes of parathyroid hormone-related peptide in chondrocytes. *Endocrinology*, **147**, 3141–3152.
57. Farndale, R.W., Buttle, D.J. and Barrett, A.J. (1986) Improved quantitation and discrimination of sulphated glycosaminoglycans by use of dimethylmethylene blue. *Biochim. Biophys. Acta*, **883**, 173–177.
58. Lakso, M., Pichel, J.G., Gorman, J.R., Sauer, B., Okamoto, Y., Lee, E., Alt, F.W. and Westphal, H. (1996) Efficient *in vivo* manipulation of mouse genomic sequences at the zygote stage. *Proc. Natl Acad. Sci. USA*, **93**, 5860–5865.
59. McLeod, M.J. (1980) Differential staining of cartilage and bone in whole mouse fetuses by Alcian blue and alizarin red S. *Teratology*, **22**, 299–301.